Trisections and the Thom Conjecture

UCLA Topology Seminar*

Fall 2018

Abstract

These are notes taken during a series of four lectures on trisections in the UCLA topology seminar. Trisections of 4-manifolds are introduced, followed by bridge trisections of surfaces in 4-manifolds. Lambert-Cole's trisections proof of the Thom conjecture is outlined in the third and fourth lectures.

Introduction

The genus of a smooth algebraic curve $\mathcal{C}_d$ of positive degree d in $\mathbb{CP}^2$ is well known to be given by

$$g(\mathcal{C}_d) = \frac{1}{2}(d-1)(d-2).$$

The Thom conjecture says that among all smoothly embedded surfaces in $\mathbb{CP}^2$ the algebraic curves are in fact genus-minimizing in their respective homology classes.

Theorem 0.1 ([KM94])**.** *Let $\mathcal{K}$ be a smoothly embedded, oriented, connected surface in $\mathbb{CP}^2$ of positive degree d. Then $g(\mathcal{K}) \geq (d-1)(d-2)/2$.*

The first proof of this result was provided by Kronheimer and Mrowka in [KM94], and is relatively short. The technical difficulty of this proof is nontrivial, however, since it makes use of the Seiberg-Witten invariants of 4-manifolds. In July of this year, Peter Lambert-Cole provided the first proof to avoid gauge theory or pseudoholomorphic curve techniques by using Gay and Kirby's trisections of 4-manifolds to reduce the Thom conjecture to the ribbon-Bennequin inequality. This is a contact-topological inequality that, according to Rudolph ([Rud93]), is equivalent to the local Thom conjecture. As with the Thom conjecture, the local Thom conjecture was first established using gauge theory, but in [Ras10], Rasmussen provides a combinatorial proof using Khovanov homology. By reducing to the local Thom conjecture, Lambert-Cole's proof provides a path to the Thom conjecture that avoids gauge theory or pseudoholomorphic curves.

These notes come from a series of talks in the UCLA topology seminar based on [GK16],[MZ17a], and [LC18]. The goal of these four talks was to quickly establish the necessary background in trisections and then to understand Lambert-Cole's new proof. The talks were organized by Sucharit Sarkar and given by Ikshu Neithalath, myself, Dave Boozer, and Mike Miller. Any errors in content or faults in exposition are my own. In particular, I've written these notes as someone learning the material rather than as an expert. The three main references are all excellent papers, written with greater detail and authority than can be found in these notes.

1 Trisections of 4-manifolds

The goal of this talk, given by Ikshu Neithalath, was to introduce trisections of 4-manifolds and the corresponding existence and uniqueness statements. Because of our later interest in the Thom conjecture, special attention was given to a trisection of $\mathbb{CP}^2$. The primary reference was [GK16].

*Notes by Austin Christian.

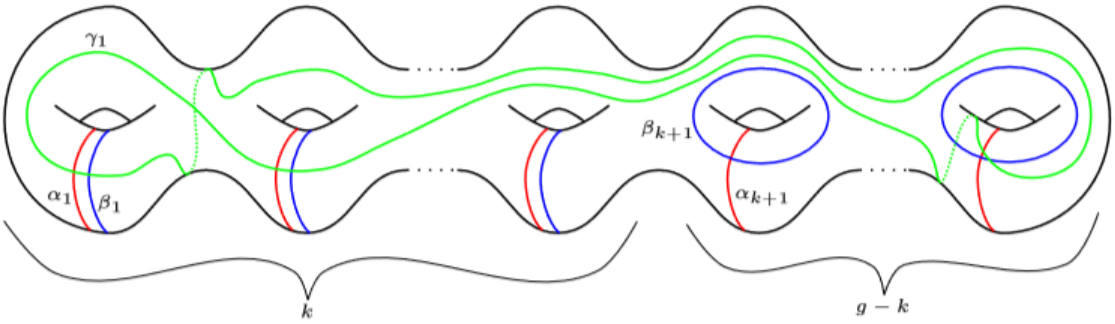

Figure 1: The α- and β-curves give the standard genus g Heegaard splitting of Y_k. Adding the rest of the γ-curves would produce a trisection diagram. Adapted from [GK16] with permission.

1.1 Introduction

Notation. For any $k \geq 1$ we write $Z_k = \natural^k(S^1 \times B^3)$ for the standard genus k 1-handlebody and $Y_k = \natural^k(S^1 \times B^2)$ for the standard genus k handlebody. For $g \geq k$ we denote by

$$Y_k = Y^+_{k,g} \cup Y^-_{k,g}$$

the standard genus g Heegaard splitting of Y_k. Here $Y^+_{k,g}$ is a surface of genus k with one boundary component and $Y^-_{k,g}$ is a surface of genus $(g-k)$ with one boundary component. See Figure 1.

Definition. Let X be a closed, connected, orientable 4-manifold. Given integers $0 \leq k \leq g$, a (g,k)-*trisection* of X is a decomposition $X = X_1 \cup X_2 \cup X_3$ such that:

1. for each i there is a diffeomorphism $\phi_i \colon X_i \to Z_k$ for some k;
2. for each i we have $\phi_i(X_i \cap X_{i+1}) = Y^+_{k,g}$ and $\phi_i(X_i \cap X_{i-1}) = Y^-_{k,g}$, with indices counted modulo 3.

Note. If X admits a (g,k)-trisection, then $\chi(X) = 2 + g - 3k$, so for a fixed 4-manifold X the genus of a trisection determines its complexity. We also see that all trisections of X have the same genus, modulo 3.

A (g,k) trisection provides us with three handlebodies $H_i = X_{i-1} \cap X_{i+1}$ and a single central surface $\Sigma = X_1 \cap X_2 \cap X_3$. We call the union $H_1 \cup H_2 \cup H_3$ the *spine* of the trisection and notice that each of these handlebodies can be represented by a cut system on Σ. Moreover, the spine determines the trisection. As with Heegaard splittings, this allows us a diagrammatic representation of trisections.

Definition. A (g,k)-*trisection diagram* is a 4-tuple $(\Sigma, \alpha, \beta, \gamma)$ consisting of a genus g surface Σ and cut systems α, β, and γ such that (Σ, α, β), (Σ, α, γ), and (Σ, β, γ) are Heegaard diagrams for $Y_1 := H_3 \cup -H_2$, $Y_2 := H_1 \cup -H_3$, and $Y_3 := H_2 \cup -H_3$, respectively[1].

The beginning of a trisection diagram can be seen in Figure 1. We can insist that (Σ, α, β) be the standard genus g Heegaard diagram of $\natural^k(S^1 \times B^2)$, so that the α- and β-curves are in the positions seen in Figure 1. In this case the g γ-curves will determine the third handlebody and thus X.

Theorem 1.1 ([GK16, Theorem 4]). *Every closed, connected, oriented 4-manifold X has a (g,k)-trisection for some $0 \leq k \leq g$. Furthermore, g and k are such that X has a handlebody decomposition with 1 0-handle, k 1-handles, $(g-k)$ 2-handles, k 3-handles, and 1 4-handle.*

Before stating the uniqueness theorem for trisections we must introduce the notion of *stabilization*. This operation replaces a trisection $X = X_1 \cup X_2 \cup X_3$ with a new decomposition $X = X'_1 \cup X'_2 \cup X'_3$. We could explain how to do this in terms of the trisection (see [GK16, Definition 8]), but it is perhaps easier to define stabilization by its effect on trisection diagrams.

[1] These should not be confused with $Y_k = \natural^k(S^1 \times B^2)$, a notation we will now abandon.

Figure 2: The genus 3 trisection diagram of S^4, adapted from [GK16] with permission.

Definition. We *stabilize* a trisection diagram $(\Sigma, \alpha, \beta, \gamma)$ by taking the connected sum with the standard $(3,1)$-trisection diagram $(\Sigma_0, \alpha_0, \beta_0, \gamma_0)$ of S^4, which is depicted in Figure 2. The result is a trisection diagram $(\Sigma \# \Sigma_0, \alpha \cup \alpha_0, \beta \cup \beta_0, \gamma \cup \gamma_0)$.

The effect of stabilization is to increase the genus by 3, and therefore increase k by 1. But, appropriately, stabilization of a trisection diagram will not change the resulting space X.

Lemma 1.2 ([GK16, Lemma 10])**.** *If $(\Sigma, \alpha, \beta, \gamma)$ is a (g,k)-trisection diagram for X, then the $(g+3, k+1)$-trisection diagram obtained by stabilization also corresponds to X.*

Theorem 1.3 ([GK16, Theorem 11])**.** *For two trisections of X, after stabilizing each some number of times, there is a diffeomorphism $h\colon X \xrightarrow{\sim} X$ carrying one trisection to the other which is isotopic to the identity.*

1.2 Examples of trisections

Example 1. The $(0,0)$-trisection diagram of S^4 consists of a sphere S^2 with no cut systems. We can realize this directly as a trisection of S^4 as follows: endow $\mathbb{R}^5 = \mathbb{R}^2 \times \mathbb{R}^3$ with a coordinate system $(r, \theta, x_1, x_2, x_3)$, where (r, θ) is the usual polar coordinate system on $\mathbb{R}^2$. Then

$$S^4 = \{(r, \theta, x_1, x_2, x_3) | r^2 + x_1^2 + x_2^2 + x_3^2 = 1\}.$$

We have a projection $p\colon S^4 \to D^2 \subset \mathbb{R}^2$ given by truncating the last three coordinates, and we may divide D^2 into three equal sectors as

$$\begin{aligned} R_1 &= \{(r,\theta) | 0 \le r \le 1, 0 \le \theta \le 2\pi/3\} \\ R_2 &= \{(r,\theta) | 0 \le r \le 1, 2\pi/3 \le \theta \le 4\pi/3\} \\ R_3 &= \{(r,\theta) | 0 \le r \le 1, 4\pi/3 \le \theta \le 2\pi\}. \end{aligned}$$

This subdivision lifts to S^4 by setting $X_i = p^{-1}(R_i)$, so that

$$X_i = \{(r, \theta, x_1, x_2, x_3) | r^2 + x_1^2 + x_2^2 + x_3^2 = 1, 2(i-1)\pi/3 \le \theta \le 2i\pi/3\} \simeq B^4.$$

The pairwise intersections are then $H_1 \simeq H_2 \simeq H_3 \simeq B^3$, and the triple intersection is

$$\Sigma := X_1 \cap X_2 \cap X_3 = \{(0, 0, x_1, x_2, x_3) | x_1^2 + x_2^2 + x_3^2 = 1\} \simeq S^2.$$

So we have a $(0,0)$-trisection of S^4.

Example 2. Since our goal is a discussion of the Thom conjecture, the 4-manifold in which we will be most interested is $\mathbb{CP}^2$. In [LC18], Lambert-Cole constructs a genus 1 trisection for $\mathbb{CP}^2$ using the moment map $\mu\colon \mathbb{CP}^2 \to \mathbb{R}^2$ of a Hamiltonian action. The moment map is given by

$$\mu([z_1 : z_2 : z_3]) = \left(\frac{|z_1|}{|z_1| + |z_2| + |z_3|}, \frac{|z_2|}{|z_1| + |z_2| + |z_3|} \right),$$

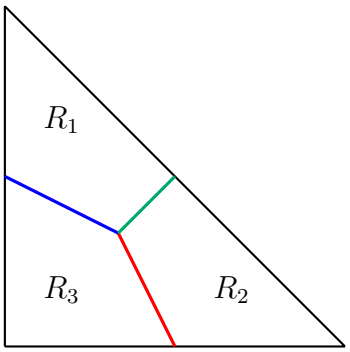

(a) Barycentric subdivision of the simplex.

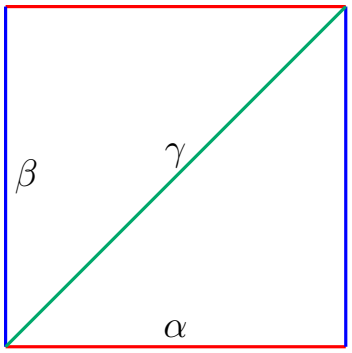

(b) The torus Σ in $z_1 z_2$-coordinates, with $z_3 = 1$.

Figure 3: The genus 1 trisection of $\mathbb{CP}^2$.

and its image is the convex hull of $(0,0)$, $(1,0)$, and $(0,1)$. Now consider the barycentric subdivision of $\mu(\mathbb{CP}^2)$. This divides $\mu(\mathbb{CP}^2)$ into three quadrilaterals with a common vertex $(1/3, 1/3)$, and the pairwise intersections of these regions are line segments connecting $(1/3, 1/3)$ to the faces of $\mu(\mathbb{CP}^2)$. See Figure 3a.

We may use μ to pull this subdivision of the simplex back to a trisection of $\mathbb{CP}^2$. We define $X_i := \mu^{-1}(R_i)$, with R_1, R_2, R_3 as labeled in Figure 3a. Some simple algebra shows that

$$\begin{aligned} X_1 &= \{[z_1 : z_2 : z_3] : |z_3|, |z_1| \leq |z_2|\}, \\ X_2 &= \{[z_1 : z_2 : z_3] : |z_2|, |z_3| \leq |z_1|\}, \\ X_3 &= \{[z_1 : z_2 : z_3] : |z_1|, |z_2| \leq |z_3|\}. \end{aligned}$$

Taking pairwise intersections produces

$$\begin{aligned} H_1 &= \{[z_1 : z_2 : z_3] : |z_1| = |z_3| \geq |z_2|\}, \\ H_2 &= \{[z_1 : z_2 : z_3] : |z_2| = |z_3| \geq |z_1|\}, \\ H_3 &= \{[z_1 : z_2 : z_3] : |z_1| = |z_2| \geq |z_3|\}. \end{aligned}$$

Finally we have the triple intersection

$$\Sigma := X_1 \cap X_2 \cap X_3 = \{[z_1 : z_2 : z_3] : |z_1| = |z_2| = |z_3|\}.$$

Notice that we can't have $z_3 = 0$ in Σ, lest all three coordinates vanish, so we scale the projective coordinates to write

$$\Sigma = \{[z_1 : z_2 : 1] || z_1| = |z_2| = 1\},$$

making it clear that Σ is a torus. We may similarly write

$$H_1 = \{[z_1 : z_2 : 1] : |z_1| = 1 \geq |z_2|\} \simeq S^1 \times D^2 \quad \text{and} \quad H_2 = \{[z_1 : z_2 : 1] : |z_2| = 1 \geq |z_1|\} \simeq D^2 \times S^1.$$

Notice that z_1 parametrizes the core circle of H_1, and z_2 parametrizes that of H_2. Projecting these circles to Σ gives the attaching curves α and β necessary to reconstruct H_1 and H_2, respectively. We may similarly identify the core circle $z_1 = z_2$ of H_3, producing an attaching curve γ in Σ. See Figure 3b.

We conclude that $X = X_1 \cup X_2 \cup X_3$ gives us a $(1,0)$-trisection of $\mathbb{CP}^2$, and in Figure 3b we have a $(1,0)$-trisection diagram. This diagram will be useful to us in later talks.

1.3 Proof sketch for the existence statement

Ikshu concluded his talk by sketching the proof of Theorem 1.1 found in [GK16, Section 3]. I won't attempt to reproduce the sketch here, but will simply say that Gay and Kirby begin by finding a Morse 2-function

$G\colon X^4 \to \mathbb{R}^2$ whose fold locus takes on a desired form. They then perform a number of Cerf moves to produce a new Morse 2-function which lifts the natural trisection of $\mathbb{R}^2$ to a trisection of X. In Section 4 of [GK16] Gay and Kirby give an alternate proof of Theorem 1.1 which uses ordinary Morse functions. Meier and Zupan build on this alternate proof when proving their existence result in [MZ17a].

2 Bridge trisections of knotted surfaces

I gave the second talk, based on [MZ17a]. The goal of this talk was to introduce the notion of *bridge position* for a knotted surface in a trisected 4-manifold and to get an idea of how to work with the resulting shadow diagrams.

2.1 Motivation

Last week we introduced trisections, which in many ways are to 4-manifolds what Heegaard diagrams are to 3-manifolds. This week we want to begin thinking about knotted surfaces in 4-manifolds, and we will attempt to continue our analogy.

In particular, consider a knot K in a 3-manifold Y. Given any Heegaard splitting of Y we may isotope K so that its intersection with each handlebody in the Heegaard splitting is a collection of unknotted arcs. We call such a decomposition of K a *bridge splitting* and say that K is in *bridge position* with respect to the Heegaard splitting. This idea has been especially fruitful when studying knots in S^3, where the *bridge number* of a knot is defined to be the smallest number of arcs in any bridge splitting of K with respect to the genus 0 Heegaard splitting of S^3.

Today we want to consider the extent to which these ideas can be generalized to 4-manifolds. Given a trisection $\mathcal{T}$ of a 4-manifold X, we will define what it means to put a knotted surface $\mathcal{K} \subset X$ into bridge position with respect to $\mathcal{T}$ and then describe a diagrammatic setup for bridge trisections.

2.2 Generalized bridge trisections

Recall that a trisection of a closed 4-manifold X partitions X into three 4-manifolds which intersect pairwise in handlebodies, and these three handlebodies meet along a central surface:

Definition. A $(g; k_1, k_2, k_3)$-*trisection* $\mathcal{T}$ of a closed 4-manifold X is a decomposition $X = X_1 \cup X_2 \cup X_3$, where

1. X_i is a 1-handlebody, i.e. $X_i = \natural^{k_i}(S^1 \times B^3)$;
2. $H_i = X_{i-1} \cap X_{i+1}$ is a handlebody, i.e. $H_i = \natural^g(S^1 \times D^2)$, for each i;
3. $\Sigma = X_1 \cap X_2 \cap X_3$ is a closed surface of genus g.

We call $H_1 \cup H_2 \cup H_3$ the *spine* of $\mathcal{T}$ and we say that $\mathcal{T}$ is a (g, k)-trisection if $k = k_i$ for each i.

Using a trisection to cut up our ambient manifold will also divide an embedded surface $\mathcal{K} \subset X$ into smaller pieces. As was the case with knots in a 3-manifold, we expect these pieces to be relatively simple.

Definition. A *trivial* (g, b)-*tangle* is a pair (H, τ), where H is a genus g handlebody and $\tau \subset H$ is a collection of b boundary-parallel embedded arcs.

Definition. A *trivial* (k, c)-*disk tangle* is a pair $(W, \mathcal{D})$, where W is a genus k 1-handlebody and $\mathcal{D} \subset W$ is a collection of c boundary-parallel disks.

Notice that the product of a trivial tangle (H, τ) with the interval I is a trivial disk tangle, an indication that our definition is a good one. We can now specify our expectations for how a trisection should divide a surface $\mathcal{K} \subset X$.

Definition. Let $\mathcal{K}$ be a knotted surface in a closed 4-manifold X. A $(g; k_1, k_2, k_3; b; c_1, c_2, c_3)$-*generalized bridge trisection* $\mathcal{T}$ of the pair $(X, \mathcal{K})$ is a decomposition

$$(X, \mathcal{K}) = (X_1, \mathcal{D}_1) \cup (X_2, \mathcal{D}_2) \cup (X_3, \mathcal{D}_3),$$

where

1. $X = X_1 \cup X_2 \cup X_3$ is a $(g; k_1, k_2, k_3)$-trisection;
2. each $(X_i, \mathcal{D}_i)$ is a trivial (k_i, c_i)-disk tangle;
3. each $(H_i, \mathcal{D}_{i-1} \cap \mathcal{D}_{i+1})$ is a trivial (g, b)-tangle;

We will typically assume a generalized bridge trisection to be *balanced*, meaning that $k = k_i$ and $c = c_i$ for all i, in which case $\mathcal{T}$ is a (g, k, b, c)-generalized bridge trisection. We call the union

$$(H_1, \tau_1) \cup (H_2, \tau_2) \cup (H_3, \tau_3)$$

the *spine* of the generalized bridge trisection, where $\tau_i = \mathcal{D}_{i-1} \cap \mathcal{D}_{i+1}$ for each i.

Definition. Let $\mathcal{T}$ be a trisection of X given by $X = X_1 \cup X_2 \cup X_3$, and let $\mathcal{K}$ be a knotted surface in X. If

$$(X, \mathcal{K}) = (X_1, \mathcal{K} \cap X_1) \cup (X_2, \mathcal{K} \cap X_2) \cup (X_3, \mathcal{K} \cap X_3)$$

is a generalized bridge trisection then we say that $\mathcal{K}$ is in *bridge position* with respect to $\mathcal{T}$.

In [MZ17b] Meier and Zupan showed that all knotted surfaces in the 4-sphere S^4 can be isotoped into bridge position with respect to any trisection of S^4. In [MZ17a] this result was extended to all closed 4-manifolds.

Theorem 2.1 ([MZ17a, Theorem 1.1])**.** *Let X be a 4-manifold with trisection $\mathcal{T}$. Any knotted surface $\mathcal{K}$ in X can be isotoped into bridge position with respect to $\mathcal{T}$.*

Notice that the Euler characteristic of a surface $\mathcal{K}$ is easy to read off from the complexity of a generalized bridge trisection for $\mathcal{K}$.

Lemma 2.2 ([MZ17a, Lemma 2.5])**.** *Suppose that $\mathcal{K} \subset X$ is in bridge position with respect to a trisection $\mathcal{T}$. Then*

$$\chi(\mathcal{K}) = c_1 + c_2 + c_3 - b.$$

Proof. If $(X, \mathcal{K})$ is a $(g; k_1, k_2, k_3; b; c_1, c_2, c_3)$-generalized bridge trisection then the components of $\mathcal{K}$ induce a cell decomposition with $2b$ 0-cells, $3b$ 1-cells, and $c_1 + c_2 + c_3$ 2-cells. □

Now let $\mathcal{K} \subset X$ be a knotted surface with n connected components. In light of the above lemma, we say that a (g, k, b, n)-generalized bridge trisection for $(X, \mathcal{K})$ is *efficient* with respect to the underlying trisection $\mathcal{T}$, because such a generalized bridge trisection minimizes b, assuming $\mathcal{K}$ and $\mathcal{T}$ are fixed. Also note that in the case of a (g, k, b, c)-generalized bridge trisection the genus g and the Euler characteristic $\chi(X)$ determine k, as we saw in Ikshu's talk. Lemma 2.2 tells us that the bridge number b determines c, so we may sometimes call a balanced trisection a (g, b)-generalized bridge trisection.

Theorem 2.3 ([MZ17a, Theorem 1.2])**.** *Let $\mathcal{K} \subset X$ be a not-necessarily-connected knotted surface. Then $(X, \mathcal{K})$ admits an efficient generalized bridge trisection with respect to some trisection of X.*

So we have an existence statement for generalized bridge trisections, and even for efficient generalized bridge trisections (though in the latter we don't get to specify $\mathcal{T}$). The uniqueness statement has not yet been settled, but Meier and Zupan conjecture that, just as the uniqueness statement for trisections requires both stabilization and destabilization, generalized bridge trisections will use both *perturbation* and *unperturbation* moves. See [MZ17a].

Conjecture 2.4 ([MZ17a, Conjecture 1.5])**.** *Any two generalized bridge trisections for a pair $(X, \mathcal{K})$ that induce isotopic trisections of X can be made isotopic after a sequence of elementary perturbation and unperturbation moves.*

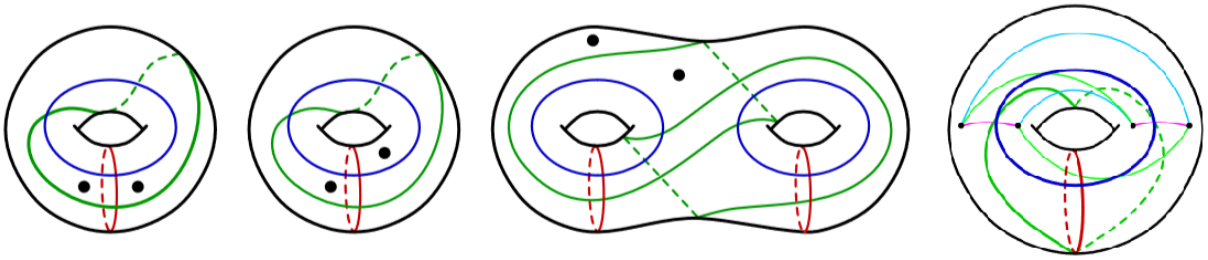

Figure 4: Trisection diagrams for $(\mathbb{CP}^2, \mathbb{CP}^1)$, $(\mathbb{CP}^2, \mathcal{C}_2)$, $(S^2 \times S^2, S^2 \times \{*\})$, and $(\mathbb{CP}^2, \mathbb{RP}^2)$. Adapted from [MZ17a] with permission.

2.3 Shadow diagrams

Recall that a trisection is determined by its spine; the same is true of a generalized bridge trisection. To see that this is so one may first show that any unlink in the boundary of a 1-handlebody bounds a unique (up to isotopy rel the unlink) collection of trivial disks in the 1-handlebody. Then from the spine $(H_1, \tau_1) \cup (H_2, \tau_2) \cup (H_3, \tau_3)$ of a generalized bridge trisection we may take pairs of tangles to produce unlinks in ∂X_i and thus reproduce the trivial disk systems.

Lemma 2.5 ([MZ17a, Corollary 2.4]). *A generalized bridge trisection is uniquely determined by its spine.*

The upshot of this lemma is a diagrammatic calculus for generalized bridge trisections. In particular, by producing a two-dimensional visual representation of the spine — one that is not unlike a multi-pointed Heegaard diagram — we in fact determine the generalized bridge trisection. We begin by defining *curve-and-arc systems*.

Definition. Let (H, τ) be a trivial tangle, so that each arc $\tau_i \in \tau$ admits a *bridge disk* $\Delta_i \subset H$ whose boundary is the union of τ_i and an arc $\overline{\tau}_i$ in ∂H. We call the arc $\overline{\tau}_i$ a *shadow* or *shadow arc* for τ_i. A *curve-and-arc system* (α, a) *determining* (H, τ) is a collection of pairwise disjoint simple closed curves α and arcs a in ∂H so that α determines H and a is a collection of shadow arcs for τ.

Note that a pair of curve-and-arc systems on a closed surface Σ provides the same data as a multi-pointed Heegaard diagram, and thus determines a knot. By specifying a triple of such systems we determine a surface.

Definition. A *shadow diagram* for a generalized bridge trisection $\mathcal{T}$ is a triple $((\alpha, a), (\beta, b), (\gamma, c))$ of curve-and-arc systems on a common surface Σ determining the spine $(H_1, \tau_1) \cup (H_2, \tau_2) \cup (H_3, \tau_3)$ of $\mathcal{T}$.

Of course there are infinitely many different shadow diagrams for a given surface $\mathcal{K} \subset X$ and, continuing our analogy with Heegaard diagrams, there are also moves which may transform one such diagram into another. We won't discuss these moves here, but Meier and Zupan show that shadow diagrams are unique up to such moves:

Proposition 2.6 ([MZ17a, Proposition 3.1]). *Any two shadow diagrams for a fixed generalized bridge trisection are related by a sequence of disk-slides within the respective curve-and-arc systems.*

Example. Suppose $\mathcal{K}$ has a $(g, k, 1, c)$-bridge trisection, so that each of the trivial tangles in the spine has a single boundary-parallel arc. In this case we may assume that the three arcs have the same endpoints and simply mark these endpoints on the surface. The arc a is then the unique (up to isotopy and disk-slides) arc in $\Sigma \setminus \alpha$ connecting the two points, and likewise for b and c. So 1-bridge trisections admit *doubly-pointed trisection diagrams*. In Figure 4 we have doubly-pointed trisection diagrams for $(\mathbb{CP}^2, \mathbb{CP}^1)$, $(\mathbb{CP}^2, \mathcal{C}_2)$, and $(S^2 \times S^2, S^2 \times \{*\})$.

When the bridge number b is greater than 1 we must specify the arcs in our curve-and-arc systems. The final trisection diagram in Figure 4 corresponds to $(\mathbb{CP}^2, \mathbb{RP}^2)$, with the pink arks giving a, the light blue arcs

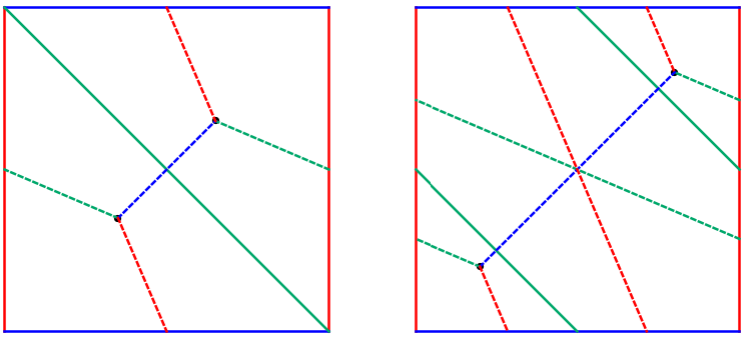

Figure 5: Torus diagrams for $(\mathbb{CP}^2, \mathbb{CP}^1)$ and $(\mathbb{CP}^2, \mathcal{C}_2)$, obtained from unfolding the diagrams seen in Figure 4.

giving b, and the light green arcs giving c. We will not attempt to justify this diagram here, but in [MZ17a, Section 3.2] Meier and Zupan explain how to realize this diagram via a double branched cover.

Eventually we would like to discuss the Thom conjecture, which concerns surfaces in $\mathbb{CP}^2$. We can draw the genus 1 trisection of $\mathbb{CP}^2$ as a fundamental square, affording us new figures for the shadow diagrams $(\mathbb{CP}^2, \mathbb{CP}^1)$ and $(\mathbb{CP}^2, \mathcal{C}_2)$ considered above. These are *torus diagrams* for $\mathbb{CP}^1$ and $\mathcal{C}_2$ in $\mathbb{CP}^2$, and can be seen in Figure 5.

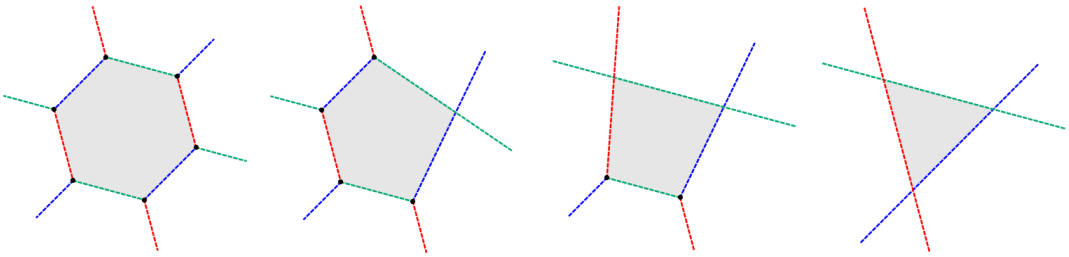

Figure 6: Hexagons in shadow diagrams can be resolved to triple intersections.

The bridge trisections we've given for $(\mathbb{CP}^2, \mathbb{CP}^1)$ and $(\mathbb{CP}^2, \mathcal{C}_2)$ witness the $d = 1$ and $d = 2$ cases of the following result[2].

Theorem 2.7 ([LCM18, Theorem 1.3]). *Let $\mathcal{C}_d$ denote the complex curve of degree d in $\mathbb{CP}^2$. The pair $(\mathbb{CP}^2, \mathcal{C}_d)$ admits a $(1, 1, (d-1)(d-2)+1, 1)$-generalized bridge trisection.*

Because $\mathcal{C}_d$ is a closed surface of genus $(d-1)(d-2)/2$, Theorem 2.7 says that complex curves in $\mathbb{CP}^2$ admit efficient generalized bridge trisections with respect to the genus 1 trisection of $\mathbb{CP}^2$.

A torus diagram that is *not* efficient, due to Peter Lambert-Cole, can be seen on the left side of Figure 7, and a justification for this diagram might be given in the next talk. In any case, we may modify this shadow diagram to obtain an efficient generalized bridge trisection for $(\mathbb{CP}^2, \mathcal{C}_3)$ with respect to the genus 1 trisection of $\mathbb{CP}^2$. In particular, consider the shaded hexagon in Figure 6, which we imagine is found in a shadow diagram for some generalized bridge trisection. By pushing the rightmost red arc through the central surface Σ we obtain the second shape seen in Figure 6. We can think of this as attaching a band in the blue-green handlebody. Next we push the topmost blue arc through Σ to obtain the third shape, and finally push the lower of the remaining green arcs through Σ. We may then isotope the fourth shape so that the

[2]This result was announced in [MZ17a] and a proof was provided in [LCM18] a few weeks after this talk. Also see the appendix of these notes.

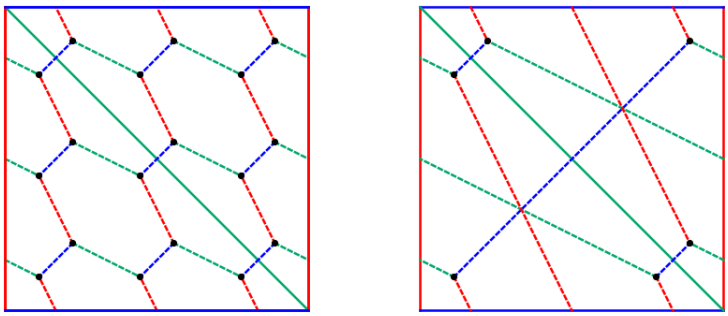

Figure 7: Two shadow diagrams for $(\mathbb{CP}^2, \mathcal{C}_3)$. On the left is a diagram for a $(1,0,9,3)$-generalized bridge splitting, and on the right is a $(1,0,3,1)$ (efficient) shadow diagram.

three remaining arcs intersect in a common point. By applying this move to two of the hexagons in Figure 7 we obtain an efficient shadow diagram for $(\mathbb{CP}^2, \mathcal{C}_3)$.

3 The Thom conjecture for surfaces in transverse bridge position

This talk was based on the first three sections of [LC18], and was given by Dave Boozer. The goal was to prove the Thom conjecture for surfaces $\mathcal{K} \subset \mathbb{CP}^2$ that are in *geometrically transverse bridge position* — a notion defined by Lambert-Cole in [LC18] — leaving the more general Thom conjecture for the final talk in the series.

3.1 Introduction

Consider the smooth algebraic curve of degree d

$$\mathcal{C}_d = \{[z_1 : z_2 : z_3] : z_1^d + z_2^d + z_3^d = 0\} \subset \mathbb{CP}^2.$$

The genus of this curve is given by $g = (d-1)(d-2)/2$, and it has long been conjectured that $\mathcal{C}_d$ is genus-minimizing among all smooth 2-manifolds in $\mathbb{CP}^2$ representing the same homology class. In 1994 Kronheimer and Mrowka raised this conjecture's status to theorem.

Theorem 0.1 ([KM94]). *Let $\mathcal{K}$ be a smoothly embedded, oriented, connected surface in $\mathbb{CP}^2$ of positive degree d. Then $g(\mathcal{K}) \geq (d-1)(d-2)/2$.*

Note. We compute the degree of $\mathcal{K}$ as its algebraic intersection number with any hyperplane of $\mathbb{CP}^2$, so the degree gives the homology class of $\mathcal{K}$: $d = [\mathcal{K}] \in H_2(\mathbb{CP}^2; \mathbb{Z}) = \mathbb{Z}$. So indeed Theorem 0.1 says that $\mathcal{C}_d$ is genus-minimizing among surfaces in its homology class.

The proof provided by Kronheimer and Mrowka uses Seiberg-Witten theory, and later proofs were found using Heegaard-Floer homology. In July of this year Peter Lambert-Cole posted [LC18], which uses the theory of trisections to reduce the Thom conjecture to a result of contact geometry known as the Bennequin inequality (at least in the case of geometrically transverse surfaces). This is the first proof of the Thom conjecture that does not make use of gauge theory or pseudoholomorphic curves.

3.2 Transverse bridge position in $\mathbb{CP}^2$

The notion of geometric transversality will be defined in terms of the $(1,0)$-trisection of $\mathbb{CP}^2$ that we've seen in the last two talks. For the sake of establishing notation we review that trisection here. With homogeneous coordinates $[z_1 : z_2 : z_3]$ on $\mathbb{CP}^2$ we let

$$X_i = \{[z_1 : z_2 : z_3] : |z_{i-1}|, |z_{i+1}| \leq 1, z_i = 1\} \simeq D^2 \times D^2 \simeq B^4$$

for $i = 1, 2, 3$. We then set

$$H_i = \{[z_1 : z_2 : z_3] : z_{i-1} = |z_{i+1}| = 1, |z_i| \leq 1\} \simeq D^2 \times S^1$$

and notice that

$$Y_i := \partial X_i = H_{i-1} \cup -H_{i+1} \simeq S^3,$$

so that $\mathbb{CP}^2 = X_1 \cup X_2 \cup X_3$ is a genus-1 trisection for $\mathbb{CP}^2$. The central surface of this trisection is given by

$$\Sigma = \bigcap_i X_i = \bigcap_i H_i = \{[z_1 : z_2 : z_3] : |z_1| = |z_2| = |z_3| = 1\}.$$

By normalizing the last coordinate we can write

$$\Sigma = \{[e^{i\alpha} : e^{i\beta} : 1]\} \simeq T^2,$$

and throughout the rest of the talk we will assume that Σ is identified with T^2 in this way. Notice that the meridians m_1 and m_2 of H_1 and H_2 are given by $\{[e^{i\alpha} : 1 : 1]\}$ and $\{[1 : e^{i\beta} : 1]\}$, respectively. The meridian m_3 of H_3 is given by $\{[e^{-i\gamma} : e^{-i\gamma} : 1]\}$, so $[m_3] = -[m_1] - [m_2]$. We also set

$$B_i = \{[z_1 : z_2 : z_3] : z_{i-1} = |z_{i+1}| = 1, z_i = 0\} \subset H_i$$

and call this the *core* of H_i, for each i. Without warning we may also slip into the notation $\alpha = m_1$, $\beta = m_2$, $\gamma = m_3$.

Given $\mathcal{K} \subset \mathbb{CP}^2$ we notice that the algebraic intersection number $[\mathcal{K}] \cdot [\Sigma]$ vanishes, since $[\Sigma]$ is trivial in $H_2(\mathbb{CP}^2, \mathbb{Z})$. Assuming that $\mathcal{K}$ is transverse to Σ this means that $\mathcal{K}$ and Σ have an even number of intersection points, so we let $b = |\mathcal{K} \cap \Sigma|/2$ and call b the *bridge index* of $\mathcal{K}$. We call the intersection points $\mathcal{K} \cap \Sigma$ the *bridge points*, and we say that $\mathcal{K}$ is in *bridge position* if for each i

1. the intersection $\mathcal{K} \cap X_i$ consists of c_i disks D^2 which can be simultaneously isotoped onto ∂X_i;
2. the intersection $K_i := \mathcal{K} \cap Y_i$ is a c_i-component unlink;
3. the intersection $\tau_i := \mathcal{K} \cap H_i$ consists of b arcs which can be simultaneously isotoped onto ∂H_i.

Notice that if $\mathcal{K}$ is in bridge position then we have a triangulation of $\mathcal{K}$ with $2b$ 0-cells, $3b$ 1-cells, and $c_1 + c_2 + c_3$ 2-cells, so $\chi(\mathcal{K}) = c_1 + c_2 + c_3 - b$.

For today's talk we will further demand that $\mathcal{K} \subset \mathbb{CP}^2$ be in *geometrically transverse bridge position*. Each tangle τ_i is contained in a solid torus H_i, and we say that $\mathcal{K}$ is in transverse bridge position if $\mathcal{K}$ is in bridge position and τ_i is transverse to all of the meridian disks of H_i. We can think of this as requiring that τ_i not backtrack (with respect to B_i) in H_i.

We will also assume, perhaps after slightly perturbing $\mathcal{K}$, that τ_i does not intersect the core B_i. This will allow us to radially project τ_i onto Σ to obtain the shadow $\overline{\tau}_i$. Of course this shadow will then depend on the position of τ_i with respect to B_i.

Examples.

1. Consider the null-homologous sphere

   $$S_r = \{[1 + x : 1 + y : e^{iz}] : x^2 + y^2 + z^2 = r^2\} \simeq S^2$$

   in $\mathbb{CP}^2$. In the interest of identifying the bridge points $S_r \cap \Sigma$ we normalize the last component and write

   $$S_r = \{[e^{-iz}(1 + x) : e^{-iz}(1 + y) : 1] : x^2 + y^2 + z^2\}.$$

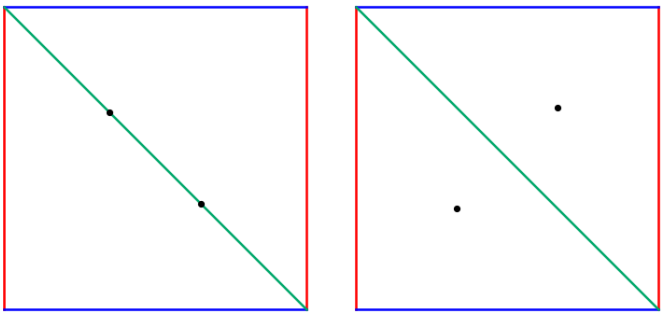

Figure 8: The surface Σ, with it the bridge points $S_r \cap \Sigma$ and $\mathbb{CP}^1 \cap \Sigma$ marked.

At the bridge points we will have $|e^{iz}(1+x)| = 1$, meaning that $|1+x| = 1$. Because x is real this will only be possible if $x = 0$, provided r is sufficiently small (say, $r < 2$). We similarly find that $y = 0$ at any bridge point, and thus conclude that $z = \pm r$. So the bridge points are given by

$$S_r \cap \Sigma = \{[e^{ir} : e^{ir} : 1], [e^{-ir} : e^{-ir} : 1]\}.$$

These bridge points are seen in Figure 8. Note that $\alpha = \beta$ for both points. We also notice that S_r is not in transverse bridge position, and indeed no null-homologous sphere in $\mathbb{CP}^2$ can be put into transverse bridge position[3].

2. Consider the degree 1 algebraic surface

$$\mathcal{C}_1 = \{[z_1 : z_2 : z_3] : z_1 + z_2 + z_3 = 0\} = \mathbb{CP}^1 \simeq S^2.$$

After normalizing we have

$$\mathcal{C}_1 = \{[z_1 : z_2 : 1] : z_1 + z_2 = -1\},$$

so we again find two bridge points:

$$\mathcal{C}_1 \cap \Sigma = \{[e^{2\pi i/3} : e^{4\pi i/3} : 1], [e^{4\pi i/3} : e^{2\pi i/3} : 1]\}.$$

We can then identify the tangles τ_1, τ_2, and τ_3 and obtain their shadows on Σ by radial projection. The resulting torus diagram is seen in Figure 5, while in Figure 8 we show only the bridge points.

We want to add a piece of data to our shadow diagrams that wasn't present in the last talk; namely, we want to determine the crossing data of intersections between shadows. We let $\overline{\tau}_i$ be the radial projection of τ_i onto Σ for each i and recall that Σ produces a Heegaard decomposition $Y_i = H_{i-1} \cup -H_{i+1}$. We view Σ with $-H_{i+1}$ in the foreground and with H_{i-1} behind Σ, so when we project the tangles to Σ we will see that $\overline{\tau}_{i+1}$ goes over $\overline{\tau}_{i-1}$ whenever these shadows intersect. Whenever $\overline{\tau}_{i-1}$ has a self-intersection, the strand that is nearer Σ will pass over the further strand, since H_{i-1} lives behind Σ. At the same time, the self-intersections of $\overline{\tau}_{i+1}$ will see the strand further from Σ pass over the nearer strand. Notice that τ_{i-1} is also contained in Y_{i+1}, and that its crossings will be reversed when we view Σ as a Heegaard surface for Y_{i+1}.

Now consider a shadow $\overline{K}_i$ of the knot K_i, using the projection $Y_i - (B_{i-1} \cup B_{i+1}) \to \Sigma$. With the crossing data determined, we can now compute the *writhe* $w_i(\overline{K}_i)$ as usual, as the signed count of crossings.

An important observation here is that by passing the tangle τ_i through the core B_i (that is, we isotope $\mathcal{K}$ so that τ_i wraps around B_i a different number of times) we can simultaneously change the homology class $[\overline{K}_i] \in H_1(\Sigma; \mathbb{Z}) = \mathbb{Z}^2$ and the writhe $w_i(\overline{K}_i)$, trading these quantities for each other. Specifically, if $[\overline{K}_i] = p[m_i] + q[m_{i+1}]$ then the surface framing on K_i induced by $\overline{K}_i$ is $w_i(\overline{K}_i) + pq$.

[3]This latter statement follows from today's result. Indeed, today we're going to show that if $\mathcal{K} \subset \mathbb{CP}^2$ can be put into transverse bridge position then $\chi(\mathcal{K}) \leq 3d - d^2$. But for a null-homologous sphere we have $\chi(\mathcal{K}) = 2$ and $d = 0$, violating this inequality. Notice that the Thom conjecture assumes $d > 0$.

3.3 A contact inequality

The contribution of [LC18] is the reduction of the Thom conjecture to the *ribbon-Bennequin inequality*. This is a generalization of the following fundamental result of contact geometry[4].

Theorem 3.1 (Bennequin inequality [Ben83],[Eli92])**.** *Let L be a transverse link in (S^3, ξ_{std}) and let Σ_L be a Seifert surface for L. Then $sl(L) \leq -\chi(\Sigma_L)$.*

A noteworthy generalization of this inequality is the *slice-Bennequin inequality*, which considers surfaces in B^4 bounding braids in S^3 and provides an upper bound for their Euler characteristics in terms of the fixed braid. This result was first established by Rudolph in [Rud93] and implies the *ribbon-Bennequin inequality*:

Theorem 3.2 (Ribbon-Bennequin inequality)**.** *Let L be a transverse link in (S^3, ξ_{std}) and let F be a ribbon surface bounded by L. Then $sl(L) \leq -\chi(F)$.*

Unlike the classical Bennequin inequality, neither slice-Bennequin nor ribbon-Bennequin currently admits a proof via standard contact-topological techniques. However, Rasmussen ([Ras10]) gives a combinatorial proof of slice-Bennequin using Khovanov homology, and therefore avoids gauge theory.

Note that if L is a transverse unlink with c components then Σ_L consists of c disjoint disks and the Bennequin inequality tells us that $sl(L) \leq -c$. This is the only case we will need today. Indeed, we will use information encoded in the shadow diagram to show that

$$d^2 - 3d - b = sl(\overline{K}_1) + sl(\overline{K}_2) + sl(\overline{K}_3). \tag{1}$$

If we assume that each K_i is a transverse link in $Y_i = S^3$ then the Bennequin inequality turns this into

$$d^2 - 3d - b \leq -(c_1 + c_2 + c_3) = -\chi(\mathcal{K}) - b,$$

so $\chi(\mathcal{K}) \leq 3d - d^2$, proving Theorem 0.1. The remainder of the talk will be devoted to establishing the equality (1).

3.4 Proof

The first trick is to put a contact structure on each of the spheres $Y_i \simeq S^3$ that agrees with the standard contact structure on S^3. We won't say exactly how this is done, but will point out that it's not done directly. Namely, Lambert-Cole produces a sequence of Stein domains $\widehat{X}_{i,N}$ contained in the interior of X_i with the property that for large enough N, $\partial\widehat{X}_{i,N} = S^3$ is C^0-close to Y_i and the field of complex tangencies on this boundary is the standard tight contact structure. For the sake of exposition we'll just pretend that (Y_i, ξ_i) is contactomorphic to (S^3, ξ_{std}).

Proposition 3.3. *Let $L \subset (Y_i, \xi_i)$ be a transverse link disjoint from the Hopf link $B_{i-1} \cup -B_{i+1}$. Let $\overline{L}$ be the projection of L onto Σ, $w(\overline{L})$ its writhe, and assume that $[\overline{L}] = p[m_{i-1}] + q[m_{i+1}]$. Then*

$$sl(\overline{L}) = w(\overline{L}) + pq - p - q \tag{2}$$

gives the self-linking number of $\overline{L}$.

Proof. We'll sketch the proof. Let X be a vector field on Y_i that is transverse to Σ and vanishes near the Hopf link $B_{i-1} \cup -B_{i+1}$. This vector field determines a framed pushoff L' of $\overline{L}$, and we can use this pushoff to compute the self-linking number of $\overline{L}$. But the linking number $lk(\overline{L}, L')$ will over-count the self-linking based on the way that $\overline{L}$ links with the cores B_{i-1}, $-B_{i+1}$. Specifically,

$$sl(\overline{L}) = lk(\overline{L}, L') - lk(\overline{L}, B_{i-1}) - lk(\overline{L}, B_{i+1}) = lk(\overline{L}, L') - p - q.$$

Because L' is transverse to Σ, the linking number $lk(\overline{L}, L')$ gives the surface framing of $\overline{L}$, and we noticed above that this is $w_i(\overline{L}) + pq$. Making this substitution produces the desired equality. □

[4]The result we state was proven by Bennequin in [Ben83] before the dichotomy between tight and overtwisted contact structures had been established. In [Eli92] Eliashberg proved that the Bennequin inequality holds for all tight contact manifolds (M, ξ), and in fact this inequality is equivalent to tightness.

An important part in the proof we're presenting today is our ability to relate the homology classes $[\overline{K}_i]$ to the degree d of our knotted surface. In [LC18], the following result follows from some degree calculations[5].

Lemma 3.4 ([LC18, Corollary 2.2]). *Let $(\mathbb{CP}^2, \mathcal{K})$ be a knotted surface of degree d in bridge position, and let $\overline{K}_i$ be the shadow of the link K_i for each i. Then there are integers p, q, r such that*

$$[\overline{K}_1] = p \cdot [\alpha] + (d-q) \cdot [\beta]$$
$$[\overline{K}_2] = q \cdot [\beta] + (d-r) \cdot [\gamma]$$
$$[\overline{K}_3] = r \cdot [\gamma] + (d-p) \cdot [\alpha]$$

in $H_1(\Sigma; \mathbb{Z})$.

If we make the assumption that each link K_i is transverse in Y_i (this is no trivial assumption), then (2) tells us that

$$sl(\overline{K}_1) = w_1(\overline{K}_1) + p(d-q) - p - (d-q)$$
$$sl(\overline{K}_2) = w_2(\overline{K}_2) + q(d-r) - q - (d-r)$$
$$sl(\overline{K}_3) = w_3(\overline{K}_3) + r(d-p) - r - (d-p).$$

Summing these yields

$$sl(\overline{K}_1) + sl(\overline{K}_2) + sl(\overline{K}_3) = w_1(\overline{K}_1) + w_2(\overline{K}_2) + w_3(\overline{K}_3) + d(p+q+r-3) - (pq+qr+rp), \tag{3}$$

so we turn our attention to computing $w_1(\overline{K}_1) + w_2(\overline{K}_2) + w_3(\overline{K}_3)$. For this we note the algebraic intersection numbers

$$\langle [\alpha], [\beta] \rangle = 1, \quad \langle [\alpha], [\gamma] \rangle = -1, \quad \text{and} \quad \langle [\beta], [\gamma] \rangle = 1,$$

since $[\gamma] = -[\alpha] - [\beta]$. Then

$$\begin{aligned} \langle [\overline{K}_1], [\overline{K}_2] \rangle &= \langle p[\alpha] + (d-q)[\beta], q[\beta] + (d-r)[\gamma] \rangle \\ &= pq - p(d-r) + (d-q)(d-r) = d^2 - d(p+q+r) + (pq+qr+rp). \end{aligned}$$

On the other hand, since $K_1 = \tau_1 - \tau_2$ and $K_2 = \tau_2 - \tau_3$, we can compute the algebraic intersection number $\langle [\overline{K}_1], [\overline{K}_2] \rangle$ as a signed count of $\overline{\tau}_1/\overline{\tau}_2$ intersections, $\overline{\tau}_2/\overline{\tau}_3$ intersections, and $\overline{\tau}_3/\overline{\tau}_1$ intersections. That is, we can compute this intersection number as the sum of the writhes $w_i(\overline{K}_i)$. So

$$w_1(\overline{K}_1) + w_2(\overline{K}_2) + w_3(\overline{K}_3) = d^2 - d(p+q+r) + (pq+qr+rp).$$

Substituting this into (3) yields (1), proving Theorem 0.1.

4 Algebraic transversality and the Thom conjecture

The final talk in the series was given by Mike Miller and was based on the second half of [LC18]. Its goal was to prove the Thom conjecture in the same spirit as last week's proof, but without the hypothesis of geometric transversality.

4.1 Introduction

Last week Dave showed us that the Thom conjecture holds for any surface $\mathcal{K} \subset \mathbb{CP}^2$ in geometrically transverse bridge position by using the tangles of a bridge trisection of $\mathcal{K}$ to produce transverse links in (S^3, ξ_{std}) and then applying the ribbon-Bennequin inequality. An ideal goal for this talk would then be to show that every surface can be isotoped into geometrically transverse bridge position, but we will see that this is not true. Instead, we will relax the condition of geometric transversality to that of *algebraic* transversality and then attempt to emulate the proof given by Dave last week. We will again reduce the Thom conjecture to a ribbon-Bennequin inequality, though the failure of geometric transversality will cause the relevant links to live in $\#_k(S^1 \times S^2, \xi_{std})$ rather than (S^3, ξ_{std}).

[5] From this result it's easy to come up with an algorithm that produces a torus diagram for a surface of degree d in $\mathbb{CP}^2$ with bridge index d^2 that contains lots of hexagons. See the appendix.

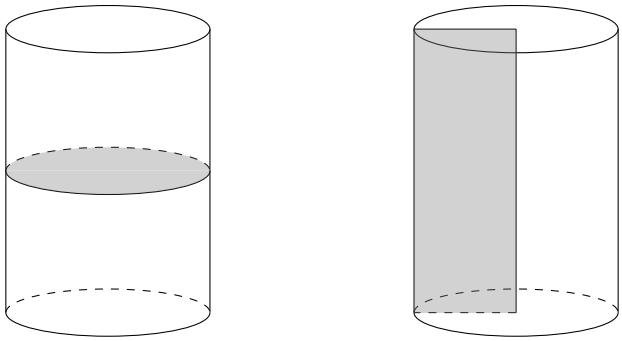

Figure 9: On the left, a foliation of H_i by holomorphic disks. On the right, a relative open book decomposition of H_i. These correspond to two notions of positivity for tangles in H_λ.

4.2 Algebraic transversality

Throughout this section we take $(\mathbb{CP}^2, \mathcal{K})$ to be in general position with respect to the $(1,0)$-trisection of $\mathbb{CP}^2$. We denote the handlebodies of this trisection by H_i and use τ_i, K_i for the tangles and knots determined by $\mathcal{K}$. Each H_i is a solid torus and thus admits polar coordinates $(r_{i+1}, \theta_i, \theta_{i+1})$, and we choose these so that $\ker(d\theta_{i+1})$ determines a foliation of H_i by disks $\{*\} \times D^2$. The notion of geometric transversality discussed last week requires that the tangle $\tau_i \subset H_\lambda$ be transverse to these disks, which can be thought of as prohibiting backtracking with respect to the S^1-component of $H_i = S^1 \times D^2$. This week we'll relax this condition so that arcs in τ_i are allowed to backtrack, so long as there is net positive movement in the S^1-direction.

Definition. A surface $(\mathbb{CP}^2, \mathcal{K})$ is *algebraically transverse* if for each arc $\tau_{i,j}$ in τ_i we have

$$\int_{\tau_{i,j}} d\theta_{i+1} > 0,$$

for each i.

Any surface in algebraically transverse bridge position can be put into geometrically transverse position with regular homotopies, but we'll see that this cannot be done by isotopy. While algebraic transversality is perhaps less desirable than geometric transversality, it has the helpful feature of being attainable.

Proposition 4.1 ([LC18, Proposition 4.4])**.** *Let $(\mathbb{CP}^2, \mathcal{K})$ be an embedded, oriented, connected surface of positive degree. Then $\mathcal{K}$ can be isotoped into algebraically transverse bridge position.*

So the surfaces of interest to us can be assumed to be algebraically transverse, but not geometrically so. It would therefore be helpful to identify any obstructions to isotoping a surface from algebraically transverse bridge position into geometrically transverse bridge position. A description of the obstruction will require the notion of *braided* tangles in the handlebodies H_i.

Definition. We will say that a tangle $\tau \subset H_i$ is *braided* if the tangle is everywhere positively transverse to the pages $F_{i,\theta} := \{\theta_i = \theta\}$ of the relative open book decomposition depicted in Figure 9. In particular, τ is disjoint from the binding $B_i = \{r_{i+1} = 0\}$.

As is the case with knots, any tangle can be isotoped into a braid, and the proof is essentially the same as that of Alexander's theorem.

Proposition 4.2 ([LC18, Proposition 4.5])**.** *Let $\tau \subset H_i$ be a tangle. There is an isotopy after which τ will be braided.*

So we may assume that any tangle $\tau \subset H_i$ of interest to us both braided and algebraically transverse, and we'd like to know whether this tangle can be made geometrically transverse. Lambert-Cole constructs a tangle for which the answer to this question is no. This tangle is relatively simple, and we will also see that it is the primary obstacle to geometric transversality.

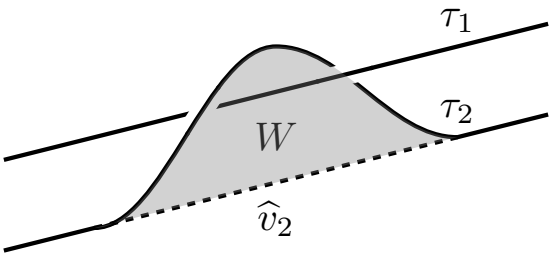

Figure 10: A simple clasp.

Definition. A *simple clasp* is a tangle $\tau = \{\tau_1, \tau_2\}$ in H_i and a disk $W \subset H_i$ such that

1. τ is algebraically transverse and braided, and τ_1 is geometrically transverse;
2. W intersects τ_1 transversely in one point;
3. $\partial W = \widehat{v}_2 \cup \widehat{\tau}_2$, where $\widehat{\tau}_2$ is a connected subarc of τ_2 and $\widehat{v}_2$ is geometrically transverse.

The notion that simple clasps are the only obstructions to geometric transversality can be made precise.

Proposition 4.3 ([LC18, Proposition 4.8])**.** *Let τ be an algebraically transverse, braided tangle in H_i. After a sequence of isotopies and bridge stabilizations we may assume that each arc of τ is either geometrically transverse and braided or one of two arcs in a simple clasp.*

From Figure 10 it is clear that a simple clasp is regular homotopic to a pair of arcs τ_1 and $(\tau_2 - \widehat{\tau}_2) \cup \widehat{v}_2$. For each i we let L_i denote the geometrically transverse link obtained by homotoping each simple clasp of K_i in this way.

4.3 Proof sketch

This final proof of the Thom conjecture will require the ribbon-Bennequin inequality for transverse links in the contact manifold[6] $\#_k(S^1 \times S^2, \xi_{std})$. We obtain this inequality by moving our problems back to (S^3, ξ_{std}).

Lemma 4.4 ([LC18, Lemma 5.2])**.** *Let $L \subset \#^k(S^1 \times S^2, \xi_{std})$ be a transverse link and let F be a ribbon surface bounded by L. There is a transverse link $L' \subset (S^3, \xi_{std})$ that bounds a ribbon surface F' with $sl(L') = sl(L)$ and $\chi(F') = \chi(F)$.*

The idea for proving Lemma 4.4 is this: if we perform Legendrian surgery on $\#_k(S^1 \times S^2, \xi_{std})$ along a k-component Legendrian unlink U whose i^{th} component is smoothly isotopic to the i^{th} factor of $S^1 \times \{*\}$ then we obtain (S^3, ξ_{std}). By isotoping U and invoking the Legendrian realization principle we may further demand that U be disjoint from F and then let L', F' be the images of L, F in (S^3, ξ_{std}) after Legendrian surgery. We may then check that the self-linking number and Euler characteristic have not changed. An immediate corollary is that the ribbon-Bennequin inequality holds for $\#_k(S^1 \times S^2, \xi_{std})$.

Corollary 4.5 ([LC18, Theorem 5.3])**.** *Let $L \subset \#^k(S^1 \times S^2, \xi_{std})$ be a transverse link and let F be a ribbon surface bounded by L. Then $sl(L) \leq -\chi(F)$.*

Now consider the links $K := K_1 \sqcup K_2 \sqcup K_3$ and $L := L_1 \sqcup L_2 \sqcup L_3$. While L is geometrically transverse, it is not clear that either of these links is ribbon. We will fix this with some surgery and banding. Recall from last week that each $Y_i = H_{i-1} \cup -H_{i+1}$ has been given a contact structure ξ_i. We set

$$(Y, \xi) := (Y_1, \xi_1) \sqcup (Y_2, \xi_2) \sqcup (Y_3, \xi_3),$$

so that if there are a total of n simple clasps in $H_1 \sqcup H_2 \sqcup H_3$ then there are $2n$ simple clasps in Y. Now for each of the simple clasps in H_i we choose a point $x \in H_i$ in a tubular neighborhood of the disk of the clasp,

[6] We put the k in the subscript of the connect sum to indicate that this is a *contact* connected sum.

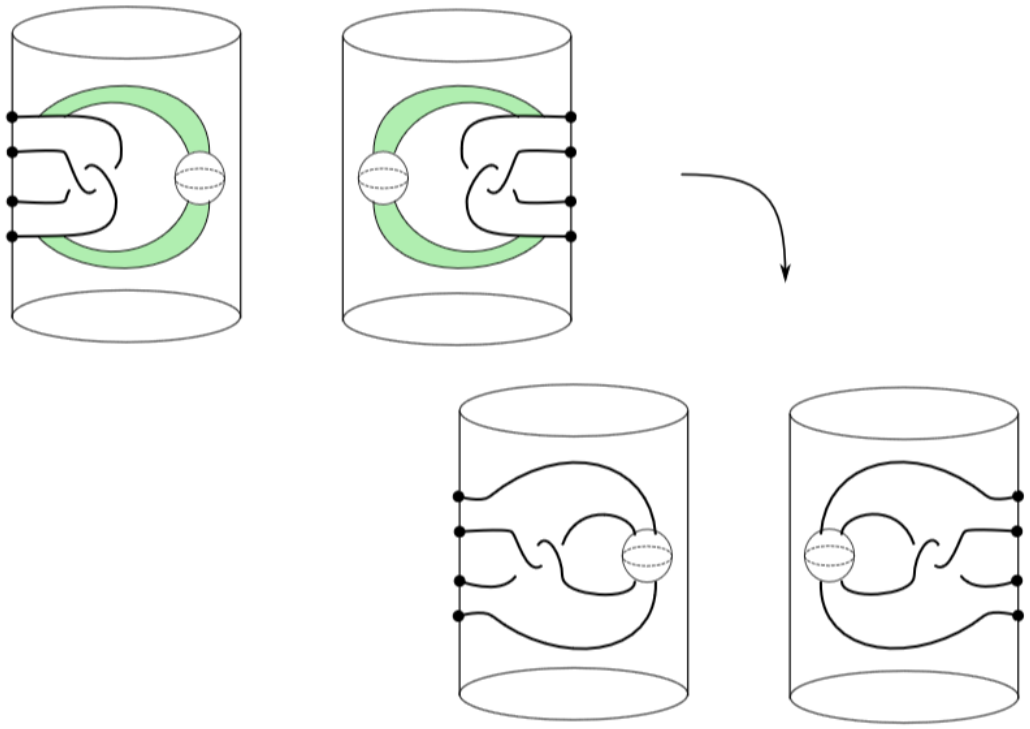

Figure 11: Bands which we attach to a simple clasp and its mirror. The result is a four-component tangle. Adapted from [LC18] with permission.

and we let $\overline{x} \in -H_i$ be the corresponding point in the mirror. Finally we perform surgery on Y along each of the 0-spheres $\{x \cup \overline{x}\}$ to obtain the contact manifold $(\tilde{Y}, \tilde{\xi})$.

Finally we return to the links K, L. Near each simple clasp $\tau \subset H_i$ of K we may attach two bands running across the 2-sphere resulting from $\{x \cup \overline{x}\}$ and connecting τ to its mirror in $-H_i$. The result of band surgery on τ is a 4-component tangle, and we attach similar bands to the link L that is regular homotopic to K. See Figure 4.6. We denote by $\tilde{K}$ and $\tilde{L}$ the links that result from resolving the $2n$ bands we have described. Lambert-Cole shows that these are the links we'd hoped for, with $\tilde{K}$ being ribbon. Moreover, Lambert-Cole specifies the Euler characteristic of a ribbon surface for $\tilde{K}$ and the self-linking number of $\tilde{L}$.

Proposition 4.6 ([LC18, Propositions 6.3 and 6.4])**.** *Let $\tilde{K}$, $\tilde{L}$ be the links obtained from K and L by band attachment. Then $\tilde{K}$ and $\tilde{L}$ are isotopic and*

1. *The link $\tilde{K}$ bounds a ribbon surface F with $\chi(F) = c_1 + c_2 + c_3 - 2n$.*
2. *The link $\tilde{L}$ admits a transverse representative with self-linking number $sl(\tilde{L}) = d^2 - 3d - b + 2n$.*

The Thom conjecture will now follow from a simple calculation. Consider an embedded, oriented, connected surface $\mathcal{K} \subset \mathbb{CP}^2$ of degree $d > 0$. Up to isotopy, $\mathcal{K}$ will be in $(1, 0; b, c_1, c_2, c_3)$ bridge position. We may further assume that $\mathcal{K}$ is in algebraically transverse bridge position, with n simple clasps. Proposition 4.6 uses $\mathcal{K}$ and its simple clasps to produce a transverse link $\tilde{L}$ in $\#_k(S^1 \times S^2, \xi_{std})$ with self-linking number

$$sl(\tilde{L}) = d^2 - 3d - b + 2n$$

which bounds a ribbon surface F with Euler characteristic $c_1 + c_2 + c_3 - 2n$. The ribbon-Bennequin inequality for $\#_k(S^1 \times S^2, \xi_{std})$ then takes the form

$$d^2 - 3d - b + 2n \leq 2n - (c_1 + c_2 + c_3).$$

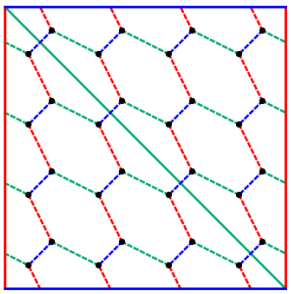

(a) A torus diagram for $\mathcal{C}_4$.

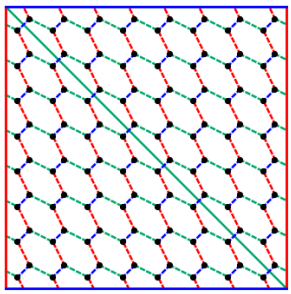

(b) A torus diagram for $\mathcal{C}_8$.

Figure 12: Torus diagrams for curves in $\mathbb{CP}^2$.

That is, $d^2 - 3d \leq b - (c_1 + c_2 + c_3)$. From Lemma 2.2 we recall that $\chi(\mathcal{K}) = c_1 + c_2 + c_3 - b$, so in fact $\chi(K) \leq 3d - d^2$, as desired.

Appendix A Torus diagrams for surfaces of fixed degree

In this appendix we want to deduce from Lemma 3.4 a simple algorithm for producing a torus diagram for a surface $\mathcal{K}$ of degree d in $\mathbb{CP}^2$. Following the preparation of this section, a much better exposition of this algorithm was provided by Lambert-Cole and Meier in [LCM18, Section 4.3].

In a way we'll be using Lemma 3.4 backwards. We will present a torus diagram $(T^2, (\alpha, a), (\beta, b), (\gamma, c))$, where $(T^2, \alpha, \beta, \gamma)$ is the $(1, 0)$-trisection diagram for $\mathbb{CP}^2$, which satisfies the equations

$$\begin{aligned}[b \cup c] &= 0 \cdot [\alpha] + d \cdot [\beta] \\ [c \cup a] &= 0 \cdot [\beta] + d \cdot [\gamma] \\ [a \cup b] &= 0 \cdot [\gamma] + d \cdot [\alpha].\end{aligned}$$

in $H_1(T^2; \mathbb{Z})$. Lemma 3.4 then tells us that the surface $\mathcal{K} \subset \mathbb{CP}^2$ must be of degree d.

The algorithm for producing $(T^2, (\alpha, a), (\beta, b), (\gamma, c))$ is quite simple. We first depict T^2 as a quotient of $[0, 1] \times [0, 1]$ in the usual way, with α vertical, β horizontal, and γ diagonal. With d fixed we then add a $d \times d$ grid of pairs of bridge points. Each pair is arranged along a positive-slope diagonal, with d rows of pairs and d columns of pairs. In particular, we may write

$$p_k^{i,j} := \left(\frac{3 + 6i + (-1)^k}{6d}, \frac{3 + 6i + (-1)^k}{6d} \right)$$

for $1 \leq i, j \leq d$ and $k = 0, 1$. Then for each choice of i, j, $p_0^{i,j}$ is connected to $p_1^{i,j}$ by an arc from b, connected to $p_1^{i,j+1}$ by an arc from a, and connected to $p_1^{i+1,j}$ by an arc from c. The $d = 4$ and $d = 8$ cases (with arc systems) can be seen in Figure 12. Each of the arc systems consists of d^2 arcs, with b connecting the points in each of the pairs we have produced. Each of the d columns of bridge points has its adjacent pairs connected by arcs in a, and each of the d rows has its adjacent pairs connected by arcs in c.

Now consider the homology class $[b \cup c]$. The link $b \cup c$ has d components, each of which is itself homologous to β. So $[b \cup c] = d[\beta]$, as desired. Similarly, $c \cup a$ and $a \cup b$ have d components, homologous to γ and α, respectively, so we have the desired homology relations. So the knotted surface associated to our torus diagram has degree d.

Notice that this torus diagram will typically be (very) inefficient. An efficient bridge trisection of $\mathcal{C}_d$ will have bridge number $(d - 1)(d - 2) + 1$, while ours has bridge number d^2. However, our torus diagram also

has lots of hexagons, giving us an opportunity to apply the simplification technique depicted in Figure 6. Specifically, each hexagon that we simplify in our torus diagram will remove 6 bridge points, decreasing our bridge number by 3. In the torus diagram produced by our algorithm we see $d-1$ pairwise disjoint hexagons along the positive-slope diagonal. Simplifying these will give us a bridge trisection of $\mathcal{K}$ with respect to the $(1,0)$-trisection of $\mathbb{CP}^2$ that has bridge number

$$d^2 - 3(d-1) = (d-1)(d-2) + 1,$$

as desired.

References

[Ben83] Daniel Bennequin. Entrelacements et equations de Pfaff. *Astérique*, 107:87–161, 1983.

[Eli92] Yakov Eliashberg. Contact 3-manifolds twenty years since J. Martinet's work. *Ann. Inst. Fourier (Grenoble)*, 42(1-2):165–192, 1992.

[GK16] David Gay and Robion Kirby. Trisecting 4–manifolds. *Geom. Topol.*, 20(6):3097–3132, 2016.

[KM94] PB Kronheimer and TS Mrowka. The genus of embedded surfaces in the projective plane. *Math. Res. Lett*, 1(6):797–808, 1994.

[LC18] Peter Lambert-Cole. Bridge trisections in $\mathbb{CP}^2$ and the Thom conjecture. *arXiv preprint arXiv:1807.10131*, 2018.

[LCM18] Peter Lambert-Cole and Jeffrey Meier. Bridge trisections in rational surfaces. *arXiv preprint arXiv:1810.10450*, 2018.

[MZ17a] Jeffrey Meier and Alexander Zupan. Bridge trisections of knotted surfaces in 4–manifolds. *arXiv preprint arXiv:1710.01745*, 2017.

[MZ17b] Jeffrey Meier and Alexander Zupan. Bridge trisections of knotted surfaces in S^4. *Trans. Amer. Math. Soc.*, 369(10):7343–7386, 2017.

[Ras10] Jacob Rasmussen. Khovanov homology and the slice genus. *Invent. Math.*, 182(2):419–447, 2010.

[Rud93] Lee Rudolph. Quasipositivity as an obstruction to sliceness. *Bull. Amer. Math. Soc.*, 29(1):51–59, 1993.